Journal for ImmunoTherapy of Cancer

Tumor MHC class I expression alters cancer-associated myelopoiesis driven by host NK cells

Shi Yong Neo,[1,2] Xu Jing,[3] Le Tong,[1] Dongmei Tong,[4] Juan Gao,[3,5] Ziqing Chen,[1,6] Mireia Cruz De Los Santos,[1] Nutsa Burduli,[7] Sabrina De Souza Ferreira,[1] Arnika Kathleen Wagner,[7] Evren Alici,[7] Charlotte Rolny,[1] Yihai Cao,[3] Andreas Lundqvist [1]

To cite: Neo SY, Jing X, Tong L, *et al*. Tumor MHC class I expression alters cancer-associated myelopoiesis driven by host NK cells. *Journal for ImmunoTherapy of Cancer* 2022;**10**:e005308. doi:10.1136/jitc-2022-005308

► Additional supplemental material is published online only. To view, please visit the journal online (http://dx.doi.org/10.1136/jitc-2022-005308).

SYN and XJ contributed equally.

SYN and XJ are joint first authors.

Accepted 25 September 2022

For numbered affiliations see end of article.

Correspondence to
Dr Andreas Lundqvist;
Andreas.Lundqvist@ki.se

ABSTRACT

Downregulation of MHC class I (MHCI) molecules on tumor cells is recognized as a resistance mechanism of cancer immunotherapy. Given that MHCI molecules are potent regulators of immune responses, we postulated that the expression of MHCI by tumor cells influences systemic immune responses. Accordingly, mice-bearing MHCI-deficient tumor cells showed reduced tumor-associated extramedullary myelopoiesis in the spleen. Depletion of natural killer (NK) cells abrogated these differences, suggesting an integral role of immune-regulatory NK cells during tumor progression. Cytokine-profiling revealed an upregulation of TNF-α by NK cells in tumors and spleen in mice-bearing MHCI expressing tumors, and inhibition of TNF-α enhanced host myelopoiesis in mice receiving adoptive transfer of tumor-experienced NK cells. Our study highlights a critical role of NK cells beyond its identity as a killer lymphocyte and more importantly, the potential host responses to a localized tumor as determined by its MHCI expression.

KEY MESSAGES

⇒ Enhanced extramedullary myelopoiesis in the spleen is prominent in mice-bearing MHC class I-expressing tumors.
⇒ Tumor-experienced natural killer cells contribute to myelopoiesis via the production of TNF-α.

INTRODUCTION

Cancer is an inflammatory disease that affects systemic hematopoietic responses. Tumor-derived factors can drive myelopoiesis resulting in the accumulation of immature myeloid cells to support tumor growth and interference with antitumor immune responses.[1 2] Moreover, the frequency of peripheral blood granulocyte–monocyte progenitors (GMPs) correlates with tumor progression and predict worse survival.[3]

Natural killer (NK) cells are not only implicated in the surveillance and eradication of cancer but also in the cross-talk with myeloid cells, including dendritic cells, to favor antitumor immune responses.[4] As means of immune evasion, the downregulation of tumor MHC class I (MHCI) can result in resistance to immune checkpoint inhibition, but at the same time, potentially implicate susceptibility to NK cell-mediated killing.[5–7] NK cells have demonstrated therapeutic efficacy in the setting of adoptive transfer in acute myeloid leukemia, with clinical responses correlating to the persistence of infused NK cells in peripheral blood and in the bone marrow.[8–10]

Given the apparent role of MHCI in shaping host NK cell responses, this study sought to explore the influence of tumor MHCI expression not only on NK cell functions but also on the immunological and hematological responses in tumor-bearing hosts.

METHODS

Detailed methods are listed in online supplemental information.

In vivo experiments

At day 0, 0.2×10^6 wild-type (WT) or *B2M*-knockout (KO) 4T1 cells were injected into the mammary fat pad of Balb/cAnNCrl mice. For RMA/S, RMA, and B16F10, tumor cells were injected subcutaneously on day 0 into the right flank of C57BL/6 mice at 1×10^6, 0.1×10^6 and 0.1×10^6 cells, respectively. For NK cell depletion in C57BL/6 mice, anti-NK1.1 was administered intraperitoneally on day −1 and once per week post tumor inoculation. Tumors and spleen were collected and analyzed on day 14 for B16F10 and day 21 for 4T1, respectively. In vivo studies were approved by the Swedish board of Agriculture (8525-2020, 6197-2019).

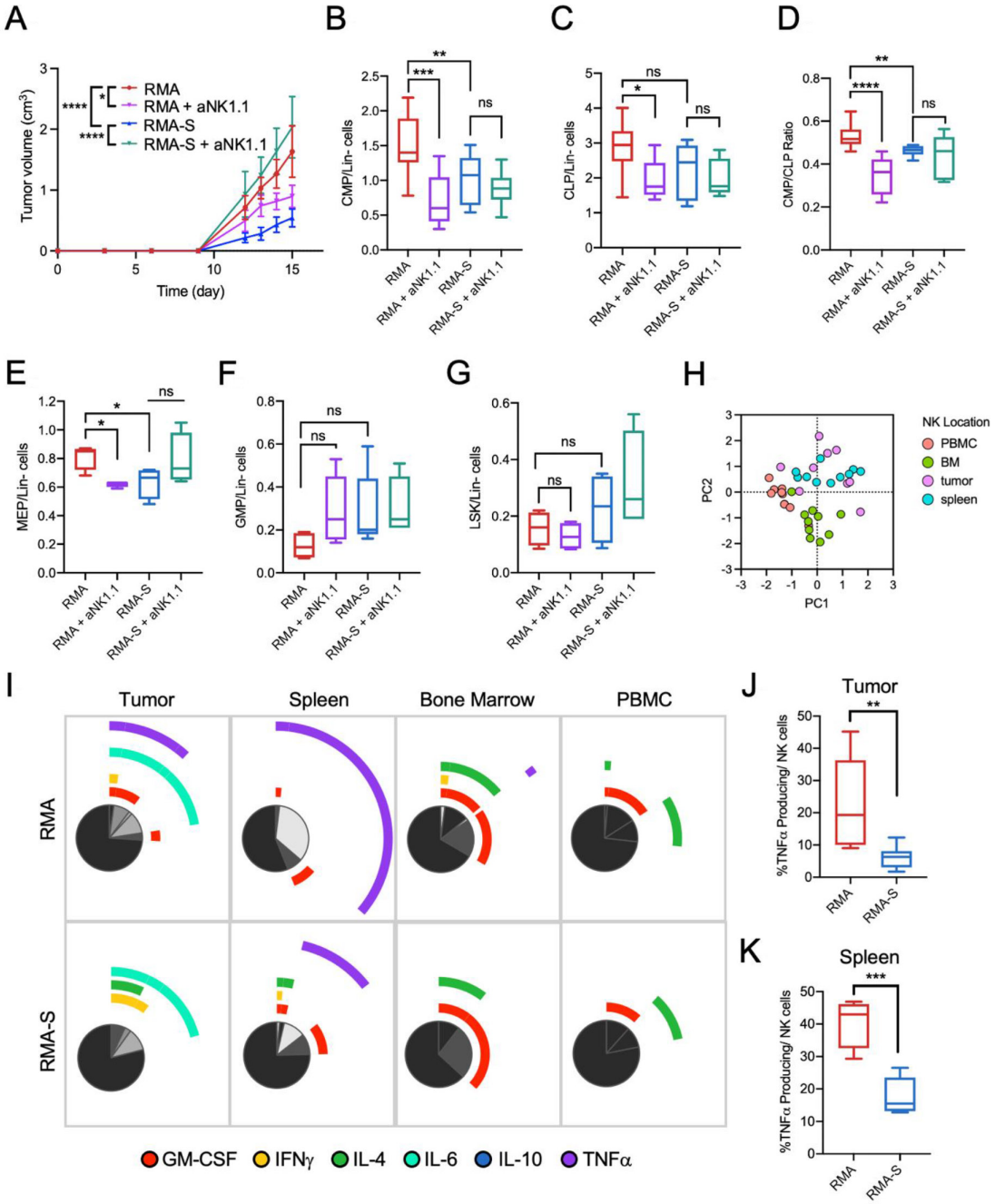

Figure 1 Tumor MHCI expression and NK cells drive extramedullary myelopoiesis in the spleen. Tumor and spleen tissues were harvested from RMA-bearing and RMA/S-bearing C57BL/6 mice 15 days post tumor inoculation. (A) Progression of RMA and RMA/S (MHCI-deficient) syngeneic tumors in untreated mice or NK cell-depleted mice. One-way ANOVA with multiple comparisons at individual time points was used to test for significance. Frequencies of (B) common myeloid progenitor (CMP) and (C) common lymphoid progenitor (CLP) within lineage-negative live cells (Lin-cells) in spleen of RMA and RMA/S tumor-bearing mice. (D) CMP to CLP ratio in spleen of RMA and RMA/S tumor-bearing mice with or without NK cell depletion. Frequencies of (E) megakaryocytic-erythroid progenitor (MEP), (F) granulocyte-monocyte progenitor (GMP) and (G) LSK (lineage-, Sca1+, cKIT+) cells within Lin-cells in spleen of RMA and RMA/S tumor-bearing mice (A–G), n=4 per group. (H) PCA analysis of NK cell cytokine production profile based on flow cytometry of samples isolated from RMA and RMA/S-bearing mice. (I) Annotated pie charts for cytokine production profiles of NK cells residing in different locations of RMA and RMA/S-bearing mice. Frequencies of <5% are not shown. (J) frequencies of TNFα-producing NK cells within RMA and RMA/S tumors. (K) Frequencies of TNFα-producing NK cells in the spleen of RMA-bearing and RMA/S-bearing mice (D–G), n=5 per group. All data are presented in tukey's boxplots except for (A, H, I). *p<0.05, **p<0.01, ***p<0.001 and ****p<0.0001. ANOVA, analysis of variance; MHCI, Major Histocompatibility Complex (MHC) class I; ns, non-significant; NK, natural killer.

Colony formation assay and myeloid output assay

Colony formation unit (CFU) with splenocytes were performed accordingly to a previously reported study.[11] Cells from colony cultures were harvested for phenotypic analysis by flow cytometry.

Statistics

Unless stated otherwise, data were analyzed using Graphpad Prism software by either Student's t-test (two groups) or one-way ANOVA with multiple comparisons.

RESULTS AND DISCUSSION

Tumor MHCI expression and NK cells drive extramedullary myelopoiesis in the spleen

Recent studies demonstrated that tumor clones with high MHCI expression display low oncogenicity but high metastatic potential.[12 13] Given that tumor MHCI expression affects immunogenicity and the immune microenvironment,[14] this study sought to investigate if tumor MHCI expression influence hematopoietic responses in tumor-bearing hosts. The RMA and TAP-deficient RMA-S lymphoma models are widely used to study tumor MHCI and NK cells interactions.[15] The progression of RMA/S tumors was significantly higher in the absence of host NK cells. In contrast, depletion of NK cells in RMA-bearing mice resulted in reduced tumor progression, suggesting a potential role of NK cells to support the progression of MHCI-positive tumors (figure 1A).

Given that tumor progression drives extramedullary myelopoiesis in the spleen,[1] frequencies of hematopoietic progenitors were analyzed. Comparing mice-bearing RMA to mice-bearing RMA/S tumors, the frequencies of CMP (common myeloid progenitor) and CMP:CLP (common lymphoid progenitor) ratio was significantly higher in mice-bearing RMA tumors even though the frequencies of CLP between these two groups were not significantly different. Notably, the differences in myelopoiesis between RMA-bearing and RMA/S-bearing mice were abrogated in NK cell-depleted mice (figure 1B,C,D). Furthermore, RMA-bearing mice show a higher frequency of MEP (megakaryocytic-erythroid progenitors) than RMA-bearing NK depleted-mice or RMA/S-bearing mice (figure 1E). Notably, since erythroid progenitors have considerable immune-suppressive capacities of T cells,[16 17] NK cell depletion may impair antitumor T cell responses through enrichment of MEPs. No significant changes were observed in the frequencies of GMP and LSK (Lineage-, Sca-1+, cKIT+ cells) (figure 1F,G). To the best of our knowledge, this study is the first to report an association between tumor MHCI expression and cancer-associated myelopoiesis.

Exposure to tumor cells alters the composition of cytokines produced by host NK cells and several of these cytokines are recognized to influence hematopoiesis.[18–20] We; therefore, hypothesized that the cytokine-profile of NK cells is involved in the observed hematopoietic alterations. Principal component analysis of the intracellular cytokine FACS (Fluorescence-Activated Cell Sorting) staining revealed that splenic NK cells share greater homology to tumorous NK cells as compared with those in bone marrow and peripheral blood (figure 1H). Compared with mice-bearing RMA/S tumors, higher frequencies of TNF-α producing splenic and tumorous NK cells was observed in mice-bearing RMA tumors (figure 1I,J,K). Since TNF-α produced by activated CD4 T cells has been shown to induce myelopoiesis,[21] it is plausible that also NK cells follow a similar underlying mechanism to contribute to myelopoiesis.

Tumor-experienced NK cells enhance systemic myelopoiesis

To investigate if tumor-experienced NK cells contribute to myelopoiesis, non-tumor-bearing mice were infused with RMA tumor-experienced NK cells (figure 2A). Similar to results obtained in RMA-bearing mice, the splenic ratio of CMP:CLP was significantly higher in mice receiving NK cells accompanied with increased proportions of immature monocytic (Ly6C^{high}) cells and polymorphonuclear (Ly6G+) cells (figure 2B,C,D). To address if TNF levels influence myelopoiesis, NK cells were coadministered with the TNF inhibitor etanercept. In spleen, a significant reduction in CMP:CLP ratio, Ly6G+ and Ly6C^{high} myeloid cells were observed compared with mice treated with NK cells alone (figure 2B,C,D). Likewise, CMP:CLP ratio within the bone marrow was elevated in mice infused with tumor-experienced NK cells which was significantly reduced in etanercept-treated mice (figure 2E). Similarly, NK cell infusion alone increased the frequency of Ly6G+ and Ly6C^{high} myeloid cells and etanercept-treated mice had similar frequencies of these myeloid cells compared with control mice (figure 2F,G). In a separate experiment, etanercept treatment alone did not significantly change CMP and CLP frequencies. However, frequencies of LSK cells, GMP, and MEP in spleen and bone marrow was altered (online supplemental figure 1A–J). Nonetheless, etanercept did not significantly influence myelopoiesis with minor differences on Ly6G+and Ly6C^{high} myeloid cells within both the bone marrow and spleen (online supplemental figure 1K to N).

To address if NK cell-induced myelopoiesis is mediated by NK cells pre-exposed to MHCI-expressing RMA but not to MHCI-deficient RMA/S cells, a separate experiment was conducted in which differential hematopoietic responses were observed (figure 2H). A significant reduction of CMP/CLP ratio was observed in bone marrow but not in spleen of mice infused with RMA/S-experienced NK cells compared with mice infused with RMA-experienced NK cells (figure 2I). Nonetheless, frequencies of Ly6C^{high} and Ly6G+myeloid cells were reduced in both spleen and bone marrow on infusion of RMA/S-experienced NK cells compared with mice infused with RMA-experienced NK cells (figure 2J and K). Collectively, differentially stimulated NK cells influence systemic hematopoiesis, where infusion of NK cells pre-exposed to MHCI-expressing target cells favor the generation of immature myeloid cells.

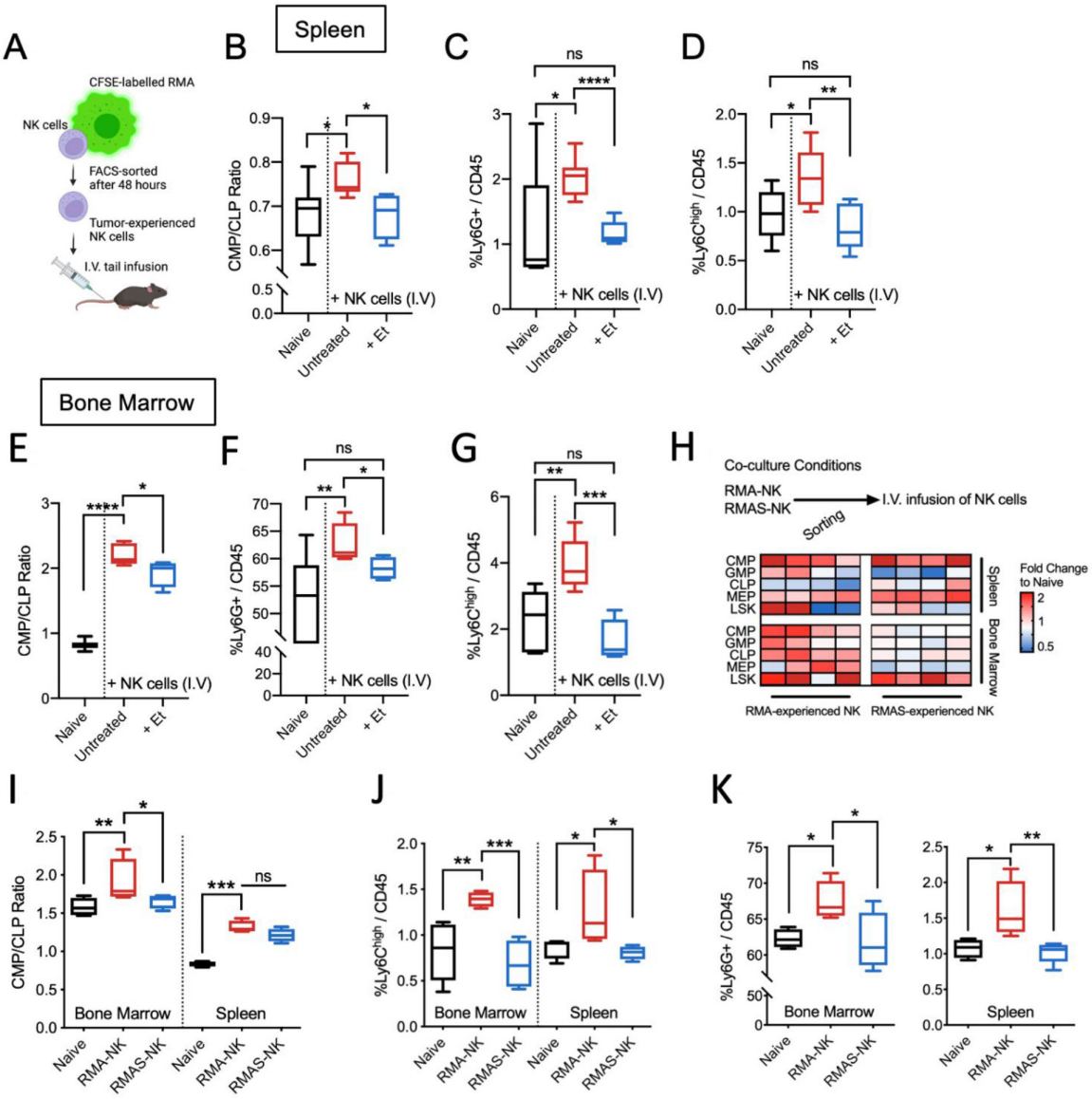

Figure 2 Infusion of tumor-experienced NK cells enhances systemic myelopoiesis without the presence of a tumor. (A) Experimental design of transfer of tumor-experienced NK cells into naïve C57BL/6 mice. Bone marrow and spleen tissues were analyzed 7 days after NK cell infusion. (B) CMP:CLP ratio, (C) frequencies of Ly6G+myeloid cells and (D) Ly6C^{high} myeloid cells within the spleen of mice 7 days after receiving NK cell infusion and etanercept (et) treatment. (E) CMP:CLP ratio, (F) frequencies of Ly6G+myeloid cells and (G) Ly6C^{high} myeloid cells within the bone marrow of mice 7 days after receiving NK cell infusion and etanercept (et) treatment. (B–G) n=5 naïve, 8 untreated with NK cell infusion, 5 with NK cell infusion and etanercept treatment given at 3 mg/kg body weight on days 0, 3, and 6. (H) Experimental design and heatmap overview of fold changes in various hmatopoietic progenitors compared with naïve mice. (I) CMP/CLP ratio within bone marrow and spleen of mice infused with RMA-experienced NK cells (RMA-NK) or RMA/S-experienced NK cells (RMA/S-NK) compared with untreated C57BL/6 mice. (J) Frequency of Ly6C^{high} myeloid cells of total CD45+ cells within bone marrow and spleen of mice infused with RMA-NK or RMA/S-NK compared with untreated C57BL/6 mice. (K) frequency of Ly6G+ myeloid cells of total CD45+ cells within bone marrow (left panel) and spleen (right panel) of mice either infused with RMA-NK or RMA/S-NK compared with untreated C57BL/6 mice. (I–K) One-way ANOVA with multiple comparisons was used to test for significance with sample size of n=4 per group. All data are presented in tukey's boxplots except for figure A and H. *p<0.05, **p<0.01, ***p<0.001 and ****p<0.0001. ANOVA, analysis of variance; CMP:CLP, common myeloid progenitor:common lymphoid progenitor; NK, natural killer; ns, non-significant.

Melanoma and breast cancer show strong association between tumor MHCI expression and enhanced splenic myelopoiesis

To corroborate our findings, we further investigated if NK cells influence myelopoiesis in other solid tumors. Even though tumor progression was not significantly different, CMP/CLP ratios, frequencies of Ly6G+and Ly6C^{high} myeloid cells were significantly reduced in the spleen of NK cell-depleted mice-bearing B16F10 tumors (online supplemental figure 2A–D) and EO771

tumors (online supplemental figure 2E–H). To investigate if the observed effects on myelopoiesis by tumor MHCI expression extend beyond lymphoma into other cancers, CRISPR was used to KO *B2M* in B16F10 melanoma and 4T1 mammary carcinoma cells prior to tumor inoculation. In both models, an initial delay in tumor progression was observed by *B2M*-KO tumors but no significant differences in tumor size was observed after 14 days (online supplemental figure 3). Compared with mice-bearing *B2M*-KO tumors, mice-bearing WT tumors showed higher splenic myelopoiesis as evidenced by higher frequencies of GMP and CMP progenitors accompanied with high GMP:CLP and CMP:CLP ratios in both B16F10 (figure 3A,B,D,E) and 4T1 models (figure 3F,G,I,J). Similar to the RMA model, no significant changes were observed in the frequencies of CLP within the spleen (figure 3C,H). Unlike the RMA model (data not shown), spleen weights were prominently lower in mice-bearing *B2M*-KO compared with mice-bearing WT tumors (figure 3K,L) which is anticipated since

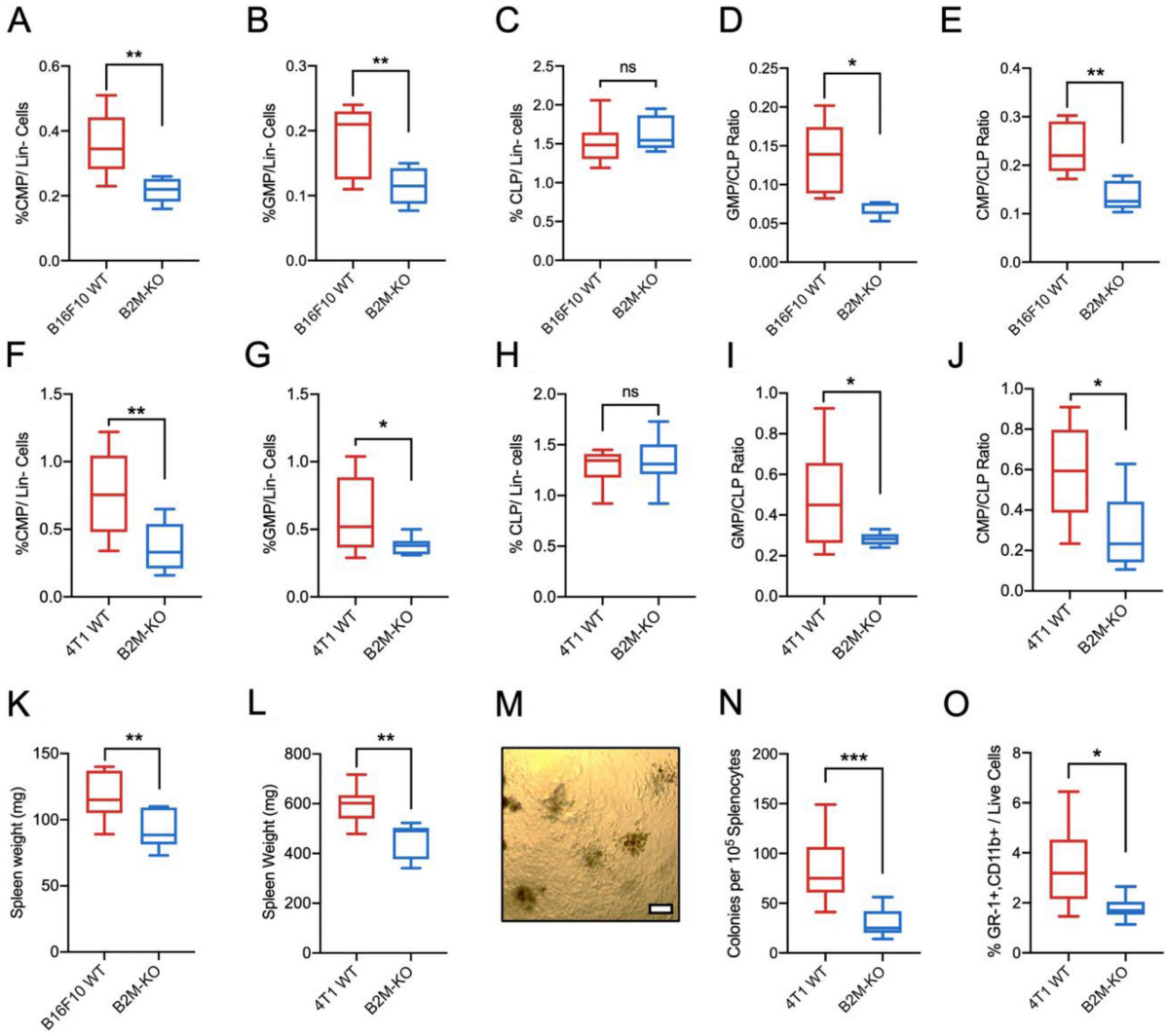

Figure 3 B16F10 and 4T1 tumor models show stronger association between tumor MHCI expression and enhanced myelopoiesis with splenomegaly. Frequencies of (A) CMP, (B) GMP and (C) CLP within lineage-negative live cells (Lin- Cells) in spleen of B16F10 tumor-bearing mice. (D) Ratio of GMP to CLP and (E) ratio of CMP to CLP in spleen of B16F10 tumor-bearing mice. Frequencies of (F) common myeloid progenitor CMP, (G) GMP and (H) CLP within lineage-negative live cells (Lin- cells) in spleen of 4T1 tumor-bearing mice. (I) Ratio of GMP to CLP and (J) ratio of CMP to CLP in spleen of 4T1 tumor-bearing mice. (K) Weight of spleen isolated from B16F10 tumor-bearing mice. (L) weight of spleen isolated from 4T1 tumor-bearing mice (A–E and K). Bone marrow and spleen tissues were harvested from B16F10 WT and B16F10 B2M-KO-bearing C57BL/6 mice 14 days post-tumor inoculation, n=6 per group (F–J and L). Bone marrow and spleen tissues were harvested from 4T1 WT and 4T1 B2M-KO-bearing BALB/c mice 21 days post tumor inoculation, n=7 per group. (M) Representative image obtained from colon formation assay under 10X objective. Scale bar denotes 100 µm. (N) Number of colonies formed by splenocytes isolated from WT or *B2M*-KO tumors after 10 days of in vitro culture. (O) Percentage of GR-1+myeloid cells from cells harvested from colony formation assay. (J–L) n=9 per group. *p<0.05, **p<0.01 and ***p<0.001. CLP, common lymphoid progenitor; CMP, common myeloid progenitor; GMPs, granulocyte–monocyte progenitors; KO, knockout; ns, non-significant; MHCI, MHC class I; NK, natural killer; WT, wild-type.

cancer-driven myelopoiesis affects splenomegaly.[22] In a CFU, splenocytes isolated from mice-bearing WT tumors formed significantly more colonies and contained higher frequency of immature myeloid cells than those isolated from mice-bearing *B2M*-KO tumors (figure 3M,N,O). Taken together, we demonstrate in different tumor models in both mice of C57BL/6 and BALB/c strains that tumor MHCI expression is associated with the host extramedullary myelopoiesis which is dependent partly on tumor progression and NK cells.

Evidently, the expression of MHCI enhances tumor immunogenicity and responsiveness to immune checkpoint therapy.[7 23] Other factors such as tumor mutational burden and the tumor microenvironment are also considered important for objective therapeutic response.[24] While cancer-associated myelopoiesis is predominantly driven by a variety of tumor-derived growth factors such GM-CSF, G-CSF, IL-6, and IL-1β,[2 25 26] this study demonstrates that the sensitivity of tumors to NK cell-mediated rejection alters the production of immune-regulatory cytokines produced by NK cells contributing to changes in myelopoiesis. Moreover, in the context of CMV infection, differential stimulation of NK cells contributes to the extramedullary expansion of TER119+ erythroid progenitors.[27] While this study uncovers a novel regulatory role of NK cells, other tumor-derived factors may also contribute in part to the differential myelopoiesis responses associated with tumor MHCI expression. From a translational perspective, strategies to increase tumor MHCI expression could potentially influence NK cell-dependent myelopoiesis that may be worthwhile investigating in future studies. Further investigating NK cell-dependent myelopoiesis in patients with hematological malignancies could be highly relevant for the development of improved therapeutics and identification of potential biomarkers. Such findings could possibly extend to other pathological disorders beyond cancer.

Author affiliations
[1]Department of Oncology-Pathology, Karolinska Institutet, Stockholm, Sweden
[2]Singapore Immunology Network SIgN, Agency for Science Technology and Research, Singapore
[3]Department of Microbiology, Tumor and Cell Biology, Karolinska Institutet, Stockholm, Sweden
[4]Centre for Innate Immunity and Infectious Disease, Hudson Institute of Medical Research, Melbourne, Victoria, Australia
[5]Department of Infectious Diseases, The Third Affiliated Hospital of Sun Yat-Sen University, Guangzhou, People's Republic of China
[6]Department of Molecular Biology, Princeton, Princeton, New Jersey, USA
[7]Department of Medicine Huddinge, Karolinska Institutet, Stockholm, Sweden

Twitter Shi Yong Neo @DrNeosy and Andreas Lundqvist @LundqvistLab

Acknowledgements We thank the animal facility (KM-F) and the flow cytometry core of Karolinska Institute for the assistance throughout the study. RMA and RMA/S were provided by Stina Wickström. We would also like to thank Apple Tay Huimin and Cui Weiyingqi for the technical assistance.

Contributors Conceptualization: SN and AL. Methodology: SN, XJ, LT, DT, JG, ZC, MCDLS, NB, SDSF and AKW. Investigation and analysis: SN, XJ, LT, DT, JG, AKW, EA, CR, YC and AL. Writing-original Draft: SN. Writing-review and editing: SN, XJ, CR and AL. Supervision and project administration: SN, AL, EA, CR and YC. Funding acquisition: AL, EA and CR.

Funding This works was supported by grants from The Swedish Cancer Society (#CAN2018/451 and #21 1524 Pj), The Cancer Research Funds of Radiumhemmet (181183 # and #211253), Stiftelsen Tornspiran, and Karolinska Institutet.

Competing interests No, there are no competing interests.

Patient consent for publication Not applicable.

Provenance and peer review Not commissioned; externally peer reviewed.

Data availability statement All data relevant to the study are included in the article or uploaded as online supplemental information.

ORCID iD
Andreas Lundqvist http://orcid.org/0000-0002-9709-2970

REFERENCES

1 Wu C, Hua Q, Zheng L. Generation of myeloid cells in cancer: the spleen matters. *Front Immunol* 2020;11:1126.
2 Innamarato P, Pilon-Thomas S. Reactive myelopoiesis and the onset of myeloid-mediated immune suppression: implications for adoptive cell therapy. *Cell Immunol* 2021;361:104277.
3 Wu W-C, Sun H-W, Chen H-T, *et al*. Circulating hematopoietic stem and progenitor cells are myeloid-biased in cancer patients. *Proc Natl Acad Sci U S A* 2014;111:4221–6.
4 Huntington ND, Cursons J, Rautela J. The cancer–natural killer cell immunity cycle. *Nat Rev Cancer* 2020;20:437–54.
5 Ljunggren H-G, Kärre K. In search of the 'missing self': MHC molecules and NK cell recognition. *Immunol Today* 1990;11:237–44.
6 Tu MM, Mahmoud AB, Makrigiannis AP. Licensed and unlicensed NK cells: differential roles in cancer and viral control. *Front Immunol* 2016;7:166.
7 Montesion M, Murugesan K, Jin DX, *et al*. Somatic HLA class I loss is a widespread mechanism of immune evasion which refines the use of tumor mutational burden as a biomarker of checkpoint inhibitor response. *Cancer Discov* 2021;11:282–92.
8 Romee R, Rosario M, Berrien-Elliott MM, *et al*. Cytokine-induced memory-like natural killer cells exhibit enhanced responses against myeloid leukemia. *Sci Transl Med* 2016;8:357ra123.
9 Dolstra H, Roeven MWH, Spanholtz J, *et al*. Successful transfer of umbilical cord blood CD34+ hematopoietic stem and progenitor-derived NK cells in older acute myeloid leukemia patients. *Clinical Cancer Research* 2017;23:4107–18.
10 Miller JS, Soignier Y, Panoskaltsis-Mortari A, *et al*. Successful adoptive transfer and in vivo expansion of human haploidentical NK cells in patients with cancer. *Blood* 2005;105:3051–7.
11 Regan-Komito D, Swann JW, Demetriou P, *et al*. GM-CSF drives dysregulated hematopoietic stem cell activity and pathogenic extramedullary myelopoiesis in experimental spondyloarthritis. *Nat Commun* 2020;11:155.
12 Garrido C, Romero I, Berruguilla E, *et al*. Immunotherapy eradicates metastases with reversible defects in MHC class I expression. *Cancer Immunol Immunother* 2011;60:1257–68.
13 Romero I, Garrido C, Algarra I, *et al*. MHC intratumoral heterogeneity may predict cancer progression and response to immunotherapy. *Front Immunol* 2018;9:102.
14 Algarra I, Garrido F, Garcia-Lora AM. MHC heterogeneity and response of metastases to immunotherapy. *Cancer Metastasis Rev* 2021;40:501–17.
15 Ljunggren HG, Kärre K. Host resistance directed selectively against H-2-deficient lymphoma variants. Analysis of the mechanism. *J Exp Med* 1985;162:1745–59.

16 Namdar A, Koleva P, Shahbaz S, *et al*. CD71+ erythroid suppressor cells impair adaptive immunity against bordetella pertussis. *Sci Rep* 2017;7:7728.
17 Long H, Jia Q, Wang L, *et al*. Tumor-induced erythroid precursor-differentiated myeloid cells mediate immunosuppression and curtail anti-PD-1/PD-L1 treatment efficacy. *Cancer Cell* 2022;40:674–93.
18 Najafi S, Ghanavat M, Shahrabi S, *et al*. The effect of inflammatory factors and their inhibitors on the hematopoietic stem cells fate. *Cell Biol Int* 2021;45:900–12.
19 Cardoso A, Martins AC, Maceiras AR, *et al*. Interleukin-10 induces interferon-γ-dependent emergency myelopoiesis. *Cell Rep* 2021;37:109887.
20 Chiba Y, Mizoguchi I, Hasegawa H, *et al*. Regulation of myelopoiesis by proinflammatory cytokines in infectious diseases. *Cell. Mol. Life Sci.* 2018;75:1363–76.
21 Al Sayed MF, Amrein MA, Bührer ED, *et al*. T-cell–secreted TNFα induces emergency myelopoiesis and myeloid-derived suppressor cell differentiation in cancer. *Cancer Res* 2019;79:346–59.
22 Wu C, Ning H, Liu M, *et al*. Spleen mediates a distinct hematopoietic progenitor response supporting tumor-promoting myelopoiesis. *J Clin Invest* 2018;128:3425–38.
23 Garrido F, Aptsiauri N, Doorduijn EM, *et al*. The urgent need to recover MHC class I in cancers for effective immunotherapy. *Curr Opin Immunol* 2016;39:44–51.
24 Lee JS, Ruppin E. Multiomics prediction of response rates to therapies to inhibit programmed cell death 1 and programmed cell death 1 ligand 1. *JAMA Oncol* 2019;5:1614–8.
25 Marigo I, Bosio E, Solito S, *et al*. Tumor-induced tolerance and immune suppression depend on the C/EBPβ transcription factor. *Immunity* 2010;32:790–802.
26 Meyer C, Sevko A, Ramacher M, *et al*. Chronic inflammation promotes myeloid-derived suppressor cell activation blocking antitumor immunity in transgenic mouse melanoma model. *Proc Natl Acad Sci U S A* 2011;108:17111–6.
27 Jordan S, Ruzsics Z, Mitrović M, *et al*. Natural killer cells are required for extramedullary hematopoiesis following murine cytomegalovirus infection. *Cell Host Microbe* 2013;13:535–45.

Supplementary Information

Methods

Generation of B2M-Knockout cells

To obtain MHCI-deficient tumor cells, we utilised CRISPR technology to knockout *B2M* (Beta-2-Microglobulin) which is a critical component of MHCI complex for antigen presentation. To generate 4T1 mammary cells with a knockout of *B2M*, gRNAs were designed to bind within either exon 1 or exon 2 of the gene using the CRISPOR algorithm (1). The gRNAs were cloned into the lentiviral expression vector lentiCRISPRv2 using BsmBI.v2 (NEB) insertion sites (2). Some gRNAs were cloned into a modified lentiCRISPRv2 plasmids, containing VQR-mutant or VRER-mutant S.p.Cas9 with altered DNA-binding specificities (3). Plasmids were verified by sequencing. Lentivirus was produced as previously described (4). Briefly, $1x10^6$ HEK293FT cells were plated into a poly-D-lysine-coated 60-mm dish (Corning) The following day, the cells were transfected with 4.8µg of the cloned lentiCRISPRv2 containing the gRNAs, 2.4µg of pMDLg/pRRE (#12251 Addgene, Cambridge, MA), 1.6µg of pRSV-REV (#12553 Addgene), and 0.8µg of phCMV-VSV-G (#8454 Addgene) using calcium phosphate transfection kit (Sigma-Aldrich) in the presence of 25µM chloroquine (Sigma-Aldrich). The medium was changed 16 hours post-transfection, and the virus particles were collected after an additional 28h, by filtering the supernatant through a 0.45µm filter and stored at -80^{o}C. 10,000 4T1 cells suspended in 2ml of RPMI medium supplemented with 10% FBS per condition were plated and allowed to adhere to a 6-well plate (Corning). Four hours post-plating, cells were transduced with 500µl of virus-containing supernatant for 6 hours in 8µg/ml protamine sulphate (Sigma Aldrich). After transduction with either sgRNA-3 or sgRNA-4, cells were cultured for four days and then stained using PE-conjugated anti-mouse H-2Kd antibody (BD Biosciences) and FACS-sorted (BD Aria fusion). FACS-sorted cells were further sub-cultured for at least a week prior to injection. To further ensure that there was no re-emergence of H-2Kd^{+} cells, cells that did not express H-2Kd were negatively selected using anti-PE microbeads (Miltenyi Biotec) (Supplementary Figure 4).

In vivo studies

All in vivo procedures were performed in strict compliance with approved ethical permits by the Swedish board of Agriculture (8525-2020, 6197-2019). Mice were housed in the animal facility with a constant temperature (20 ± 2 °C), constant humidity (50 ± 10%), and constant 12-hour day/night light cycle with food and water provided equilibrium. Any signs of body weight loss were monitored after tumor inoculation throughout. Tumor volume was monitored and measured every other day and calculated according to the standard formula (length × width^2 × 0.52). All the mice were randomly divided to each group, minimizing cage effects as potential confounder. Sample size was chosen to achieve a greater than 95% probability of identifying, by appropriate statistical analysis. Experimental outliers such as unusual tumor growth or necrotic tissue samples were excluded from analysis.

For the 4T1 metastatic mammary model, 0.2x10^6 wild-type or *B2M*-KO 4T1 cells were injected on day 0 into the mammary fat pad of 5-7 week-old female Balb/cAnNCrl mice (SCANBUR) (n=8 per group). Tumors, and spleen were collected on day 18. For FACS analysis, a part of the tumor was processed and digested with tumor dissociation kit (Miltenyi Biotech). After removal of muscles from the bones, single cells from bone marrow were then flushed by a 27G needle and syringe filled with PBS containing 10% FBS.

Female C57BL/6 mice at 7-week-old (Janvier) were used for B16F10, EO771, RMA and RMA-S experiments. 0.1x10^6 B16F10 cells were resuspended in 50µL phosphate buffered saline (PBS) and injected subcutaneously into the right flank. For EO771 model, 1x10^6 cells were injected on day 0 into the mammary fat pad of female mice. For the RMA and RMA-S models, 0.1x10^6 and 1x10^6 cells were injected subcutaneously into the right flank respectively. NK cells were depleted using conventional anti-NK1.1 depletion antibody treatment in vivo. Anti-NK1.1 neutralizing antibody (35mg/kg body weight, Mabtech) was intraperitoneally injected one day before tumor injection and then once per week. In both the B16F10 and RMA models, mice were sacrificed using a lethal dose of CO_2 after 18 days post tumor implantation.

For NK cell infusion, NK cells were isolated from a pool of four healthy murine spleens via negative selection based on manufacturer's protocol (Mouse NK cell isolation kit, Miltenyi Biotec). Purified NK cells were then co-cultured with either CFSE-labelled RMA or RMA/S cells for 48 hours, supplemented with 300 IU/ml of human IL-2 (Proleukin). NK cells were FACS-sorted (BD Aria Fusion) for purification and then intravenously injected (tail vein) at $0.5x10^6$ cells into healthy C57BL/6 mice. Etanercept (Sigma Aldrich) was administered intraperitoneally at 3mg/kg body weight on day 0,3 and 6. All mice were sacrificed after day 7.

Flow Cytometry

Single-cell suspensions of PBMC and tissue samples were washed with FACS buffer (5% FBS in PBS) before staining with antibody mixes (see Supplementary Table 1). FACS data were acquired using Novocyte Quanteon and analysed using FlowJo (BD) (Gating strategy in supplementary figure 5). For intracellular staining of cytokines, cell suspensions were treated overnight with Golgi-stop and Golgi-Plug (BD Biosciences). Intracellular staining procedures were carried out with BD Cytofix/Cytoperm^{TM} kit (BD Biosciences) with recommended protocol from manufacturer. Annotated pie charts were generated by Pestle and SPICE software developed by National Institutes of Health (NIH).

CFU and Myeloid output assay

$1x10^5$ splenocytes were cultured in 6-well plates with 1ml of MethoCult Media (Stem cell technologies). After 10 days, colonies were counted (minimum area> 10^4 μm^2) on incucyte S3 platform and flow cytometry was thereafter performed on harvested cells.

Statistics

Unless stated otherwise, data were analyzed by Graphpad Prism software by either student *t*-test (2 groups) or one-way ANOVA with multiple comparisons. Results were presented in tukey's boxplots. ns= non-significant, *p<0.05, **p<0.01, ***p<0.001 and ****p<0.0001.

References

1. Haeussler M, Schonig K, Eckert H, Eschstruth A, Mianne J, Renaud JB, et al. Evaluation of off-target and on-target scoring algorithms and integration into the guide RNA selection tool CRISPOR. Genome Biol. 2016;17(1):148.
2. Sanjana NE, Shalem O, Zhang F. Improved vectors and genome-wide libraries for CRISPR screening. Nat Methods. 2014;11(8):783-4.
3. Kleinstiver BP, Prew MS, Tsai SQ, Topkar VV, Nguyen NT, Zheng Z, et al. Engineered CRISPR-Cas9 nucleases with altered PAM specificities. Nature. 2015;523(7561):481-5.
4. Sutlu T, Nystrom S, Gilljam M, Stellan B, Applequist SE, Alici E. Inhibition of intracellular antiviral defense mechanisms augments lentiviral transduction of human natural killer cells: implications for gene therapy. Hum Gene Ther. 2012;23(10):1090-100.

114 **Supplementary Table 1.** List of antibodies used for flow cytometry

Marker	Fluorophore	Catalog#	Vendor	comments
FIXABLE LIVE/DEAD	AMCYAN	L34957	THERMO FISHER SCIENTIFIC	Dead cell marker
FIXABLE LIVE/DEAD	APC-CY7	L34975	THERMO FISHER SCIENTIFIC	Dead cell marker
CD117	BV785	135138	BIOLEGEND	
SCA-1	BV421	108127	BIOLEGEND	
CD127	ALEXA FLUOR 488	135017	BIOLEGEND	
CD34	PE-CY7	128617	BIOLEGEND	
CD16/CD32	APC	156607	BIOLEGEND	
H-2KD	PE	553566	BD BIOSCIENCES	
I-A/I-E	PERCP	107623	BIOLEGEND	
LY6G	PACIFIC BLUE	560603	BD BIOSCIENCES	
LY6C	PE	128007	BIOLEGEND	
TER-119	PE	116207	BIOLEGEND	Lineage Marker
CD45R	PE	561878	BD BIOSCIENCES	Lineage Marker
CD3	PE	553064	BD BIOSCIENCES	Lineage Marker
GR-1	PE	553128	BD BIOSCIENCES	Lineage Marker
CD11B	PE	101207	BIOLEGEND	Lineage Marker
H2Kb	BV421	116525	BIOLEGEND	
IL-4	PERCP/CY5.5	504123	BIOLEGEND	
IL-6	APC	504507	BIOLEGEND	
IL-10	PE-DAZZLE 594	505033	BIOLEGEND	
GM-CSF	PE-CY7	505411	BIOLEGEND	
CD3	PE/Fire700	100272	BIOLEGEND	
CD45	ALEXA FLUOR 700	103128	BIOLEGEND	
CD11B	PE-CY7	25-0112-82	EBIOSCIENCES	
CD11C	FITC	11-0114-82	EBIOSCIENCES	
IFNY	BV785	505837	BIOLEGEND	
TNF-A	BV605	506329	BIOLEGEND	
NK1.1	BV421	108741	BIOLEGEND	

115

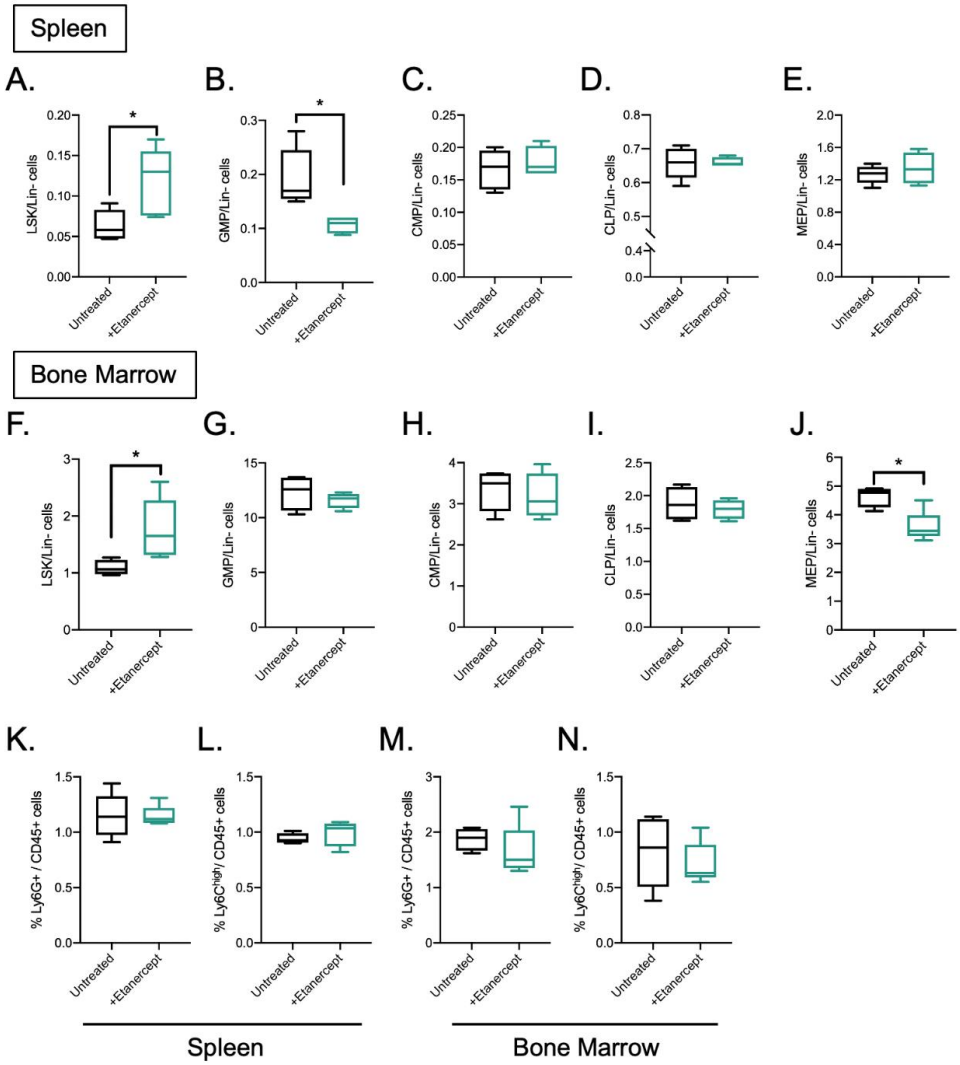

Supplementary Figure 1. Etanercept treatment alone does not influence myelopoiesis in spleen and bone marrow.

A to E, Frequencies of **(A)** LSK cells, **(B)** GMP, **(C)** CMP, **(D)** CLP and **(E)** MEP over lineage-negative cells in the spleen.
F to J, Frequencies of **(F)** LSK cells, **(G)** GMP, **(H)** CMP, **(I)** CLP and **(J)** MEP over lineage-negative cells in the bone marrow.
K and L, Frequencies of **(K)** Ly6G+ and **(L)** Ly6C^{high} myeloid cells over total CD45+ cells within the spleen.
M and N, Frequencies of **(M)** Ly6G+ and **(N)** Ly6C^{high} myeloid cells over total CD45+ cells within the bone marrow.
A to N, Comparison between untreated C57BL/6 mice (n=5) and Etanercept-treated mice (n=5) were tested for significance using student t-test. Unless indicated * for significance ($p<0.05$) otherwise, all other comparisons are not significantly different between the 2 groups.

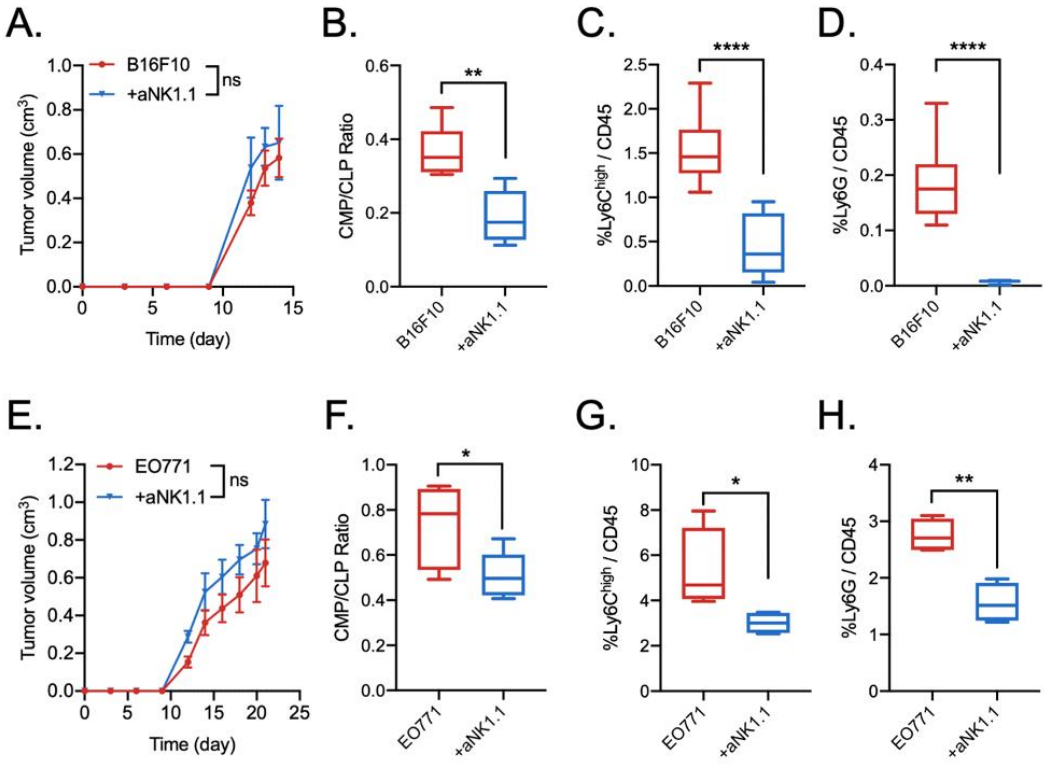

Supplementary Figure 2. NK cell depletion in tumor-bearing mice experienced decreased splenic myelopoiesis.
A, Tumor progression comparing C57BL/6 mice bearing B16F10 tumors with or without NK cell depletion.
B, Differences in CMP/CLP ratio within the spleen of B16F10-bearing mice with or without NK cell depletion.
C and D, Percentage of Ly6C^{high} and Ly6G+ myeloid cells over total CD45+ cells within the spleen of B16F10-bearing mice with or without NK cell depletion.
E, Tumor progression comparing C57BL/6 mice bearing EO771 tumors with or without NK cell depletion.
F, Differences in CMP/CLP ratio within the spleen of EO771-bearing mice with or without NK cell depletion.
G and H, Percentage of Ly6C^{high} and Ly6G+ myeloid cells over total CD45+ cells within the spleen of EO771-bearing mice with or without NK cell depletion.
A to H, NK cells were depleted using anti-NK1.1 depletion antibody in C57BL/6 mice with **(A to D)** B16F10 experiment were conducted with n=6 per group while **(E to H)** EO771 experiment was conducted with n=4 per group.
A and E, One-way ANOVA with multiple comparisons at individual timepoints was used to test for significance. ns= non-significant.
Student t-test was used to test for significance comparing untreated over NK cell-depleted mice in **(B to D)** B16F10-bearing mice and **(F to H)** EO771-bearing mice. *p<0.05, **p<0.01 and ****p<0.0001.

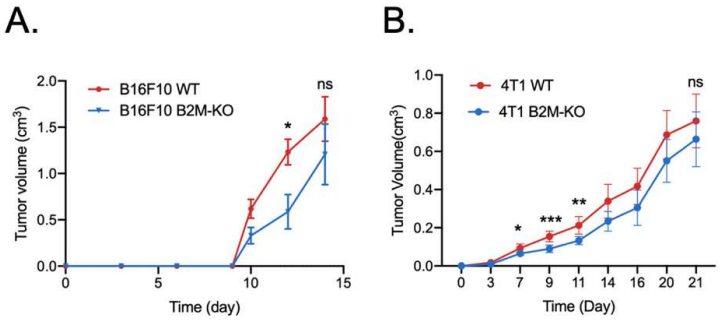

Supplementary Figure 3. Tumor progression in wild type (WT) syngeneic cell line with MHCI-deficient (B2M-KO) cells. **(A)** B16F10 cells was injected into C57BL/6 mice (n=6 per group) while **(B)** 4T1 cells were injected in BALB/c mice (n=7 per group) respectively. One-way ANOVA with multiple comparisons at individual timepoints was used to test for significance. ns= non-significant, *p<0.05, **p<0.01 and ***p<0.001.

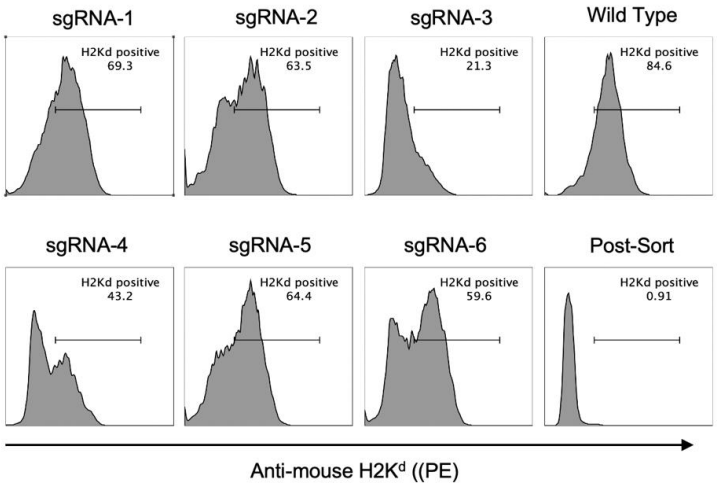

Supplementary Figure 4. CRISPR validation of 6 different sgRNA constructs for *B2M*-KO performed in 4T1 cell line. Transduced cells were negatively selected, purified and validated by flow cytometry.

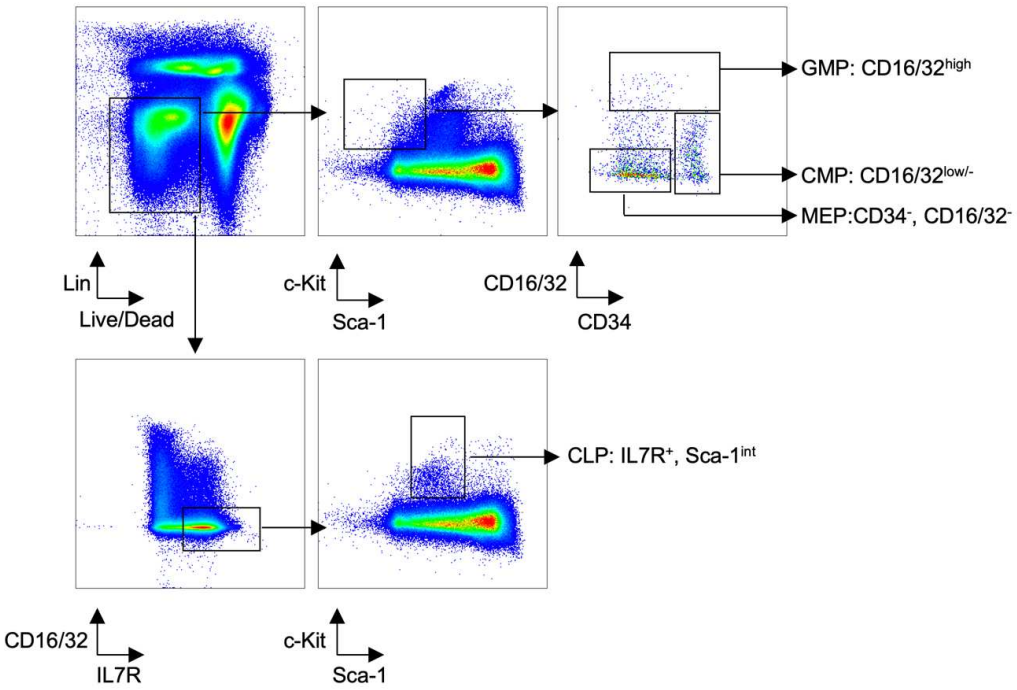

Supplementary Figure 5. Gating strategy for hematopoietic precursors for both bone marrow and spleen FACS analysis.